

Surface Chemistry

International Edition: DOI: 10.1002/anie.201706104
German Edition: DOI: 10.1002/ange.201706104On-Surface Formation of Cumulene by Dehalogenative Homocoupling of Alkenyl *gem*-Dibromides

Qiang Sun, Bay V. Tran, Liangliang Cai, Honghong Ma, Xin Yu, Chunxue Yuan, Meike Stöhr,* and Wei Xu*

Abstract: The on-surface activation of carbon–halogen groups is an efficient route to produce radicals for constructing various hydrocarbons and carbon nanostructures. To date, the employed halide precursors have only one halogen attached to a carbon atom. It is thus of interest to study the effect of attaching more than one halogen atom to a carbon atom with the aim of producing multiple unpaired electrons. By introducing an alkenyl *gem*-dibromide, cumulene products were fabricated on a Au(111) surface by dehalogenative homocoupling reactions. The reaction products and pathways were unambiguously characterized by a combination of high-resolution scanning tunneling microscopy and non-contact atomic force microscopy measurements together with density functional calculations. This study further supplements the database of on-surface synthesis strategies and provides a facile manner for incorporation of more complicated carbon scaffolds into surface nanostructures.

The recently developed on-surface synthesis strategy has gained increasing attention owing to its prospects in constructing (starting from organic monomers) covalently interlinked, extended nanostructures, which are of scientific and technological interest for future applications owing to their promising electronic properties and high mechanical stability.^[1–6] In general, most of the on-surface reactions follow pathways different from their counterparts in solution because of the effects of the surface: the reactions are confined in two dimensions and there is the possibility of catalytic surface activity.^[7–14] Consequently, unexpected reactions have been discovered in on-surface synthesis experiments,^[15–22] and thus, this strategy has opened up a way for the fabrication of a plethora of novel surface nanostructures which may be hardly obtained by traditional solution methods. Among others, the atomically precise synthesis of carbon nanostructures such as graphene nanoribbons^[23–30] and other hydrocarbons such as alkanes, dienes, and diynes has become a hot topic within the field of on-surface synthe-

sis.^[31–36] In particular, it has been demonstrated that the thermally induced dehalogenation of pre-defined C–X groups (X = halogen) provides an efficient route to produce radicals for subsequent C–C couplings on surfaces.^[14,24,27] Besides, some reactive intermediates, such as arynes,^[37] aromatic diradicals, and a highly strained ten-membered diyne^[38] have been artificially generated on surfaces by cleaving C–X bonds with the aid of STM manipulations and thereby yielding radicals. However, to the best of our knowledge, the halide precursors employed so far have only one halogen atom attached to a carbon atom, which can produce merely one unpaired electron at the carbon site. Thus, it is of particular interest to investigate dehalogenative reactions of geminal dihalide precursors on surfaces, to explore and thereby extend our fundamental understandings of on-surface C–C coupling reactions with two unpaired electrons.

Recently, we have investigated the dehalogenative homocoupling of alkenyl bromides on Cu(110).^[39] In light of this previous study, we have designed and synthesized a molecular precursor functionalized with an alkenyl *gem*-dibromide group (4-(2,2-dibromovinyl)-1,1'-biphenyl, named bBVBP), as shown in Figure 1. Herein, by the combination of high-resolution STM and nc-AFM measurements, we investigate the debromination and the subsequent C–C homocoupling reactions of alkenyl *gem*-dibromides on a Au(111) surface. We unambiguously identify from the single-bond resolved nc-AFM images the formation of *cis*- and *trans*-cumulene products having three consecutive C–C double bonds, as shown in Figure 1. These findings are explained by successive debromination reactions followed by subsequent C–C homocouplings on the basis of our DFT-based transition-state search calculations. This study extends the database of on-

[*] Q. Sun, L. Cai, H. Ma, X. Yu, Dr. C. Yuan, Prof. Dr. W. Xu
Interdisciplinary Materials Research Center, Tongji-Aarhus Joint
Research Center for Nanostructures and Functional Nanomaterials,
College of Materials Science and Engineering, Tongji University
Shanghai 201804 (P. R. China)
E-mail: xuwei@tongji.edu.cn
Dr. B. V. Tran, Prof. Dr. M. Stöhr
Zernike Institute for Advanced Materials, University of Groningen
Nijenborgh 4, 9747 AG Groningen (The Netherlands)
E-mail: m.a.stohr@rug.nl

Supporting information for this article can be found under:
<https://doi.org/10.1002/anie.201706104>.

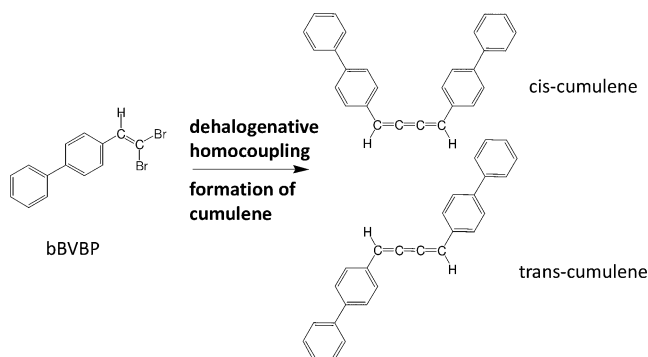


Figure 1. Illustration showing the formation of *cis*- and *trans*-cumulene products through dehalogenative C–C homocoupling reactions of the alkenyl *gem*-dibromide molecular precursor bBVBP.

surface dehalogenative C–C homocoupling reactions by introducing *gem*-dibromides. Importantly, it provides a facile manner to generate two unpaired electrons by a surface-assisted successive C–Br bond activation resulting in the formation of C–C double bonds (specifically, cumulenes in this case) based on C–C homocouplings. This is a new strategy for incorporating more complicated carbon scaffolds into tailor-made surface nanostructures.

After deposition of bBVBP molecules on Au(111) held at room temperature, we observed the formation of discrete structural motifs as well as small aggregations on the surface as shown in the overview STM image in Figure 2a. A closer

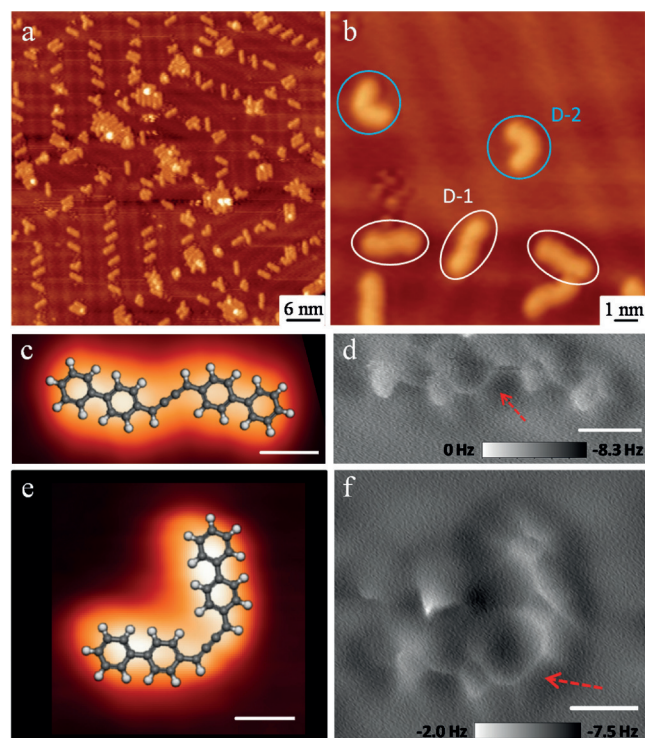


Figure 2. Formation of cumulene on Au(111). a) Overview STM image showing the formation of discrete motifs after deposition of bBVBP molecules on Au(111) at room temperature. b) Close-up STM image allowing the identification of two typical dimer structures, labeled as D-1 and D-2, respectively. Scanning parameters: $V_t = -2.1$ V, $I_t = 20$ pA. c), e) High-resolution STM images of the dimer structures D-1 and D-2, respectively, together with the equally scaled DFT relaxed models overlaid on top. d), f) Corresponding frequency shift AFM images of the two dimer structures. The red arrows indicate the cumulene groups. Scale bars: 5 Å.

inspection of the STM image allows to identify that most of the molecules reside at the fcc regions or elbow sites of the herringbone reconstruction of the Au(111) surface. The two most abundant motifs observed are shown in Figure 2b: one displays a linear shape with two lobes (labeled D-1) and the other displays a curved shape with two lobes as well (labeled D-2). Based on the STM appearances and dimensions of the two lobes, we infer that both D-1 and D-2 are composed of two bBVBP molecules. According to our previous study,^[39] such D-1 and D-2 dimers are speculated to be the products of dehalogenative C–C homocoupling reactions on the surface.

However, the bond configurations within the dimer structures cannot be precisely determined based on the STM images. Note that we occasionally observe a trimer structure exhibiting three lobes (Supporting Information, Figure S1), and a tetramer structure having four lobes (see below).

To further characterize the chemical structures of the D-1 and D-2 dimers, we utilized single-bond resolved nc-AFM imaging in conjunction with DFT calculations. First, we focus on the D-1 structure. From the high-resolution STM image and the corresponding frequency shift AFM image (Figure 2c and d, respectively), we identify that the two biphenyl groups are linked together, which confirms the formation of a dimer structure. More importantly, a sharp line with a homogeneous contrast connecting the two biphenyl groups (indicated by a red arrow in Figure 2d) can be clearly discerned. Generally, such features observed in nc-AFM images usually indicate chemical bonds within a molecule.^[40–43] Based on the above analyses, we unambiguously assign this characteristic line feature to the cumulene group having three consecutive C–C double bonds, as illustrated in the DFT relaxed model in Figure 2c. In line with D-1, we also imaged D-2 with STM and nc-AFM as shown in Figure 2e and f, respectively. We could again clearly resolve the two biphenyl groups linked together by a similar line feature (indicated by a red arrow in Figure 2f). This implies the formation of the cumulene group within the D-2 structure as well (cf. DFT relaxed model in Figure 2e). According to the isomeric configurations of D-1 and D-2, we assign D-1 to the *trans*-cumulene product, and D-2 to the *cis* one.

To further verify the formation of the cumulene group, we performed further DFT calculations to construct the relevant structural models of both *trans*- and *cis*-cumulene products on Au(111), and calculated the corresponding charge densities. As shown in Figure 3a and 3b, both cumulene products adopt flat-lying geometries on Au(111) except the slight tilt of the benzene rings with respect to each other,^[44,45] and the cumulene group adopts for both cases a linear geometry. The average molecular heights are measured to be 3.1 Å from the DFT models. It has been previously stated that the intramolecular contrast resolved by nc-AFM can be modeled by considering the charge density of the targeted molecules, because the atomic contrast is a consequence of Pauli repulsion.^[47,48] Thus, we calculated the charge density for both cumulene products adsorbed on Au(111), and the cuts along the planes parallel to the surface are shown in Figure 3c and d. From these charge density map slices, we can clearly distinguish the biphenyl groups, and more importantly, the cumulene groups exhibit a linear contrast in good agreement with their nc-AFM features. Additionally, on the basis of the optimized models, we performed the corresponding nc-AFM simulations by an online modeling software,^[46] which also agree well with our experimental results (see Figure 3e,f).

Interestingly, we also occasionally observed some tetramers consisting of four lobes on the Au surface. From the combination of high-resolution STM and the nc-AFM measurements (Figure 4a and b), we could determine that such a tetramer structure is actually composed of two *cis*-cumulene dimers. DFT calculations show that these two *cis*-cumulene dimers are stabilized by a relatively weak

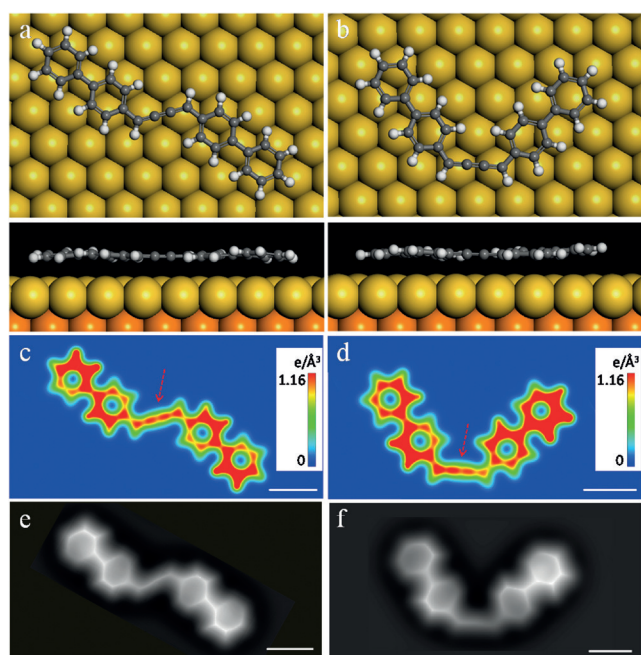


Figure 3. DFT calculations of both cumulenes on Au(111). a), b) DFT relaxed models of *trans*- and *cis*-cumulene products on Au(111). c), d) Calculated electron density maps of both products, which are cut along a plane parallel to the Au surface above the molecules. The cumulene groups are indicated by red arrows. e), f) The corresponding simulated constant-height nc-AFM images. Scale bars: 5 Å.

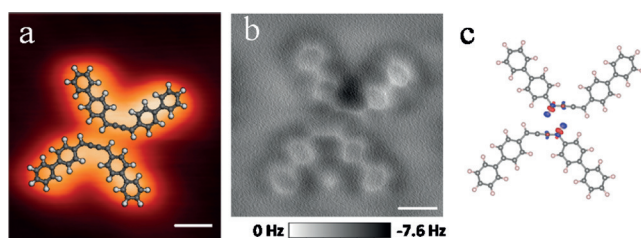


Figure 4. The tetramer structure. a), b) High-resolution STM image and the corresponding frequency shift nc-AFM image of a tetramer structure on Au(111). c) Charge density difference of the structure showing the intermolecular interactions. The isosurface value is at $0.006 \text{ e}\text{\AA}^{-3}$. Scale bars: 5 Å.

intermolecular interaction ($\text{CH}\cdots\pi$) as reflected by the charge density difference map (Figure 4c), and the binding energy is determined to be 0.18 eV. Note that it is hard to determine from the STM image alone the covalent or non-covalent character between two *cis*-cumulene dimers within this tetramer structure. Thanks to the simultaneously acquired nc-AFM image, the non-covalent feature between the two dimers could be identified. On the other hand, in comparison with the *cis*-cumulene dimer structure, it further corroborates the formation of the cumulene group on the surface.

To understand the dehalogenative homocoupling of alkenyl *gem*-dibromides from a fundamental point of view, we performed extensive calculations to explore the possible reaction pathways from molecular precursors to cumulene products on the Au(111) surface. As shown in Figure 5, we have proposed reasonable reaction pathways of the successive

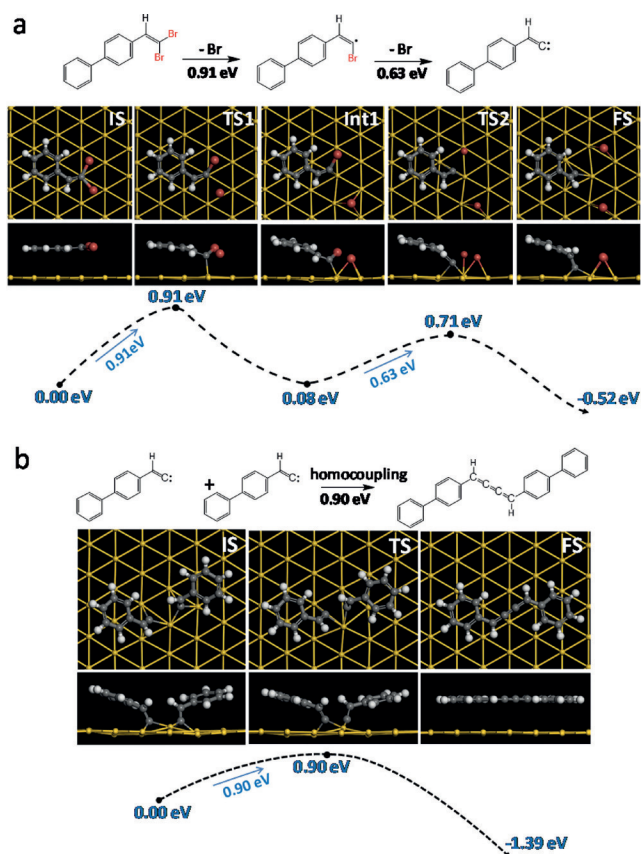


Figure 5. Reaction pathways for the formation of the *trans*-cumulene. a) The DFT-calculated reaction pathway for the successive C–Br bond activations of the simplified bBVBP molecule on Au(111). b) The DFT-calculated reaction pathway from the debrominated intermediates to a cumulene product on Au(111). The structural models of the initial (IS), transition (TS), intermediate (Int), and final states (FS) along the pathways are also shown.

C–Br bond activations followed by subsequent C–C homocouplings on the Au(111) surface (for the calculations, a simplified bBVBP molecule was used, for which the biphenyl group was replaced by a phenyl group). In the first step, a surface stabilized radical is formed by a successive splitting of two C–Br bonds. As shown in Figure 5a, the energy barriers for the successive debrominations on Au(111) are calculated to be 0.91 eV and 0.63 eV, respectively, and the whole dehalogenation reaction is exothermic by 0.52 eV. The energy barrier for the subsequent C–C homocoupling was calculated to be 0.90 eV as depicted in Figure 5b, along with a reaction energy of 1.39 eV. All of these energy barriers are in reasonable agreement with the experimental conditions and could well account for the observed formation of the cumulene products on Au(111).

In conclusion, from the combination of high-resolution UHV-STM and nc-AFM imaging together with DFT calculations, we successfully fabricated cumulene products on the Au(111) surface by introducing dehalogenative homocoupling reactions of alkenyl *gem*-dibromides. Additionally, with the help of DFT calculations we were able to suggest a reasonable reaction pathway for all the steps involved to obtain from the starting monomers to the final cumulene

products. It has been recently reported that the elusive aryne has been generated by STM tip excitation on the NaCl/Cu(111) surface and the formed aryne represents a curved cumulene resonance structure.^[37] Another comparable case is the observation of a cumulene moiety as one of the transient intermediates along an enediyne coupling and cyclization reaction.^[48] Our study sets itself apart from these results since we succeeded for the first time to create linear cumulene structures in a highly controllable fashion. More importantly, it may shed light on the fabrication of increasingly complicated carbon scaffoldings by utilizing the on-surface synthesis strategy.

Acknowledgements

The authors acknowledge financial support from the National Natural Science Foundation of China (21473123, 21622307, 51403157) as well as from Netherlands Organization for Scientific Research (NWO, Chemical Sciences, Vidi Grant No. 700.10.424) and the European Research Council (ERC-2012-StG 307760-SURFPRO).

Conflict of interest

The authors declare no conflict of interest.

Keywords: cumulenes · gem-dibromide · homocoupling · scanning tunneling microscopy · surface chemistry

How to cite: *Angew. Chem. Int. Ed.* **2017**, *56*, 12165–12169
Angew. Chem. **2017**, *129*, 12333–12337

- [1] D. G. de Oteyza, P. Gorman, Y. C. Chen, S. Wickenburg, A. Riss, D. J. Mowbray, G. Etkin, Z. Pedramrazi, H. Tsai, A. Rubio, M. F. Crommie, F. R. Fischer, *Science* **2013**, *340*, 1434.
- [2] L. Lafferentz, F. Ample, H. Yu, S. Hecht, C. Joachim, L. Grill, *Science* **2009**, *323*, 1193.
- [3] Q. Sun, C. Zhang, Z. Li, H. Kong, Q. Tan, A. Hu, W. Xu, *J. Am. Chem. Soc.* **2013**, *135*, 8448.
- [4] L. Grill, M. Dyer, L. Lafferentz, M. Persson, M. V. Peters, S. Hecht, *Nat. Nanotechnol.* **2007**, *2*, 687.
- [5] G. Franc, A. Gourdon, *Phys. Chem. Chem. Phys.* **2011**, *13*, 14283.
- [6] X. Zhang, Q. Zeng, C. Wang, *Nanoscale* **2013**, *5*, 8269.
- [7] Q. Sun, L. Cai, S. Wang, R. Widmer, H. Ju, J. Zhu, L. Li, Y. He, P. Ruffieux, R. Fasel, W. Xu, *J. Am. Chem. Soc.* **2016**, *138*, 1106.
- [8] D. Zhong, J. Franke, S. K. Podiyanchari, T. Blöchl, H. Zhang, G. Kehr, G. Erker, H. Fuchs, L. Chi, *Science* **2011**, *334*, 213.
- [9] Q. Sun, C. Zhang, H. Kong, Q. Tan, W. Xu, *Chem. Commun.* **2014**, *50*, 11825.
- [10] A. Wiengarten, K. Seufert, W. Auwärter, D. Eciija, K. Diller, F. Allegretti, F. Bischoff, S. Fischer, D. A. Duncan, A. C. Papa-georgiou, F. Klappenberger, R. G. Acres, T. H. Ngo, J. V. Barth, *J. Am. Chem. Soc.* **2014**, *136*, 9346.
- [11] N. Kocic, X. Liu, S. Chen, S. Decurtins, O. Krejčí, P. Jelínek, J. Repp, S. X. Liu, *J. Am. Chem. Soc.* **2016**, *138*, 5585.
- [12] Q. Li, B. Yang, H. Lin, N. Aghdassi, K. Miao, J. Zhang, H. Zhang, Y. Li, S. Duhm, J. Fan, L. Chi, *J. Am. Chem. Soc.* **2016**, *138*, 2809.
- [13] P. Han, K. Akagi, F. Federici Canova, H. Mutoh, S. Shiraki, K. Iwaya, P. S. Weiss, N. Asao, T. Hitosugi, *ACS Nano* **2014**, *8*, 9181.
- [14] Q. Fan, C. Wang, Y. Han, J. Zhu, W. Hierarchy, J. Kuttner, G. Hilt, J. M. Gottfried, *Angew. Chem. Int. Ed.* **2013**, *52*, 4668; *Angew. Chem.* **2013**, *125*, 4766.
- [15] H. Y. Gao, P. A. Held, M. Knor, C. Mück-Lichtenfeld, J. Neugebauer, A. Studer, H. Fuchs, *J. Am. Chem. Soc.* **2014**, *136*, 9658.
- [16] J. Liu, Q. Chen, L. Xiao, J. Shang, X. Zhou, Y. Zhang, Y. Wang, X. Shao, J. Li, W. Chen, G. Q. Xu, H. Tang, D. Zhao, K. Wu, *ACS Nano* **2015**, *9*, 6305.
- [17] Q. Sun, C. Zhang, L. Cai, L. Xie, Q. Tan, W. Xu, *Chem. Commun.* **2015**, *51*, 2836.
- [18] W. Wang, X. Shi, S. Wang, M. A. Van Hove, N. Lin, *J. Am. Chem. Soc.* **2011**, *133*, 13264.
- [19] S. Kawai, V. Haapasilta, B. D. Lindner, K. Tahara, P. Spijker, J. A. Buitendijk, P. Spijker, J. A. Buitendijk, R. Pawlak, T. Meier, Y. Tobe, A. S. Foster, E. Meyer, *Nat. Commun.* **2016**, *7*, 12711.
- [20] H. Zhou, J. Liu, S. Du, L. Zhang, G. Li, Y. Zhang, B. Z. Tang, H. J. Gao, *J. Am. Chem. Soc.* **2014**, *136*, 5567.
- [21] B. Cirera, N. Giménez-Agulló, J. Björk, F. Martínez-Peña, A. Martín-Jimenez, J. Rodríguez-Fernandez, A. M. Pizarro, R. Otero, J. M. Gallego, P. Ballester, J. R. Galan-Mascaros, D. Eciija, *Nat. Commun.* **2016**, *7*, 11002.
- [22] M. Matena, T. Riehm, M. Stöhr, T. A. Jung, L. Gade, *Angew. Chem. Int. Ed.* **2008**, *47*, 2414; *Angew. Chem.* **2008**, *120*, 2448.
- [23] P. Ruffieux, S. Wang, B. Yang, C. Sánchez-Sánchez, J. Liu, T. Dienel, L. Talirz, P. Shinde, C. A. Pignedoli, D. Passerone, T. Dumslaff, X. Feng, K. Müllen, R. Fasel, *Nature* **2016**, *531*, 489.
- [24] J. Cai, P. Ruffieux, R. Jaafar, M. Bieri, T. Braun, S. Blankenburg, M. Muoth, A. P. Seitsonen, M. Saleh, X. Feng, K. Müllen, R. Fasel, *Nature* **2010**, *466*, 470.
- [25] H. Zhang, H. Lin, K. Sun, L. Chen, Y. Zagranyski, N. Aghdassi, S. Li, Q. Duhm, D. Zhong, Y. Li, K. Müllen, H. Fuchs, L. Chi, *J. Am. Chem. Soc.* **2015**, *137*, 4022.
- [26] Y. C. Chen, D. G. De Oteyza, Z. Pedramrazi, C. Chen, F. R. Fischer, M. F. Crommie, *ACS Nano* **2013**, *7*, 6123.
- [27] T. A. Pham, B. V. Tran, M. T. Nguyen, M. Stöhr, *Small* **2017**, *13*, 1603675.
- [28] S. Kawai, S. Saito, S. Osumi, S. Yamaguchi, A. S. Foster, P. Spijker, E. Meyer, *Nat. Commun.* **2015**, *6*, 8098.
- [29] A. Kimouche, M. M. Ervasti, R. Drost, S. Halonen, A. Harju, P. M. Joensuu, J. Sainio, P. Liljeroth, *Nat. Commun.* **2015**, *6*, 10177.
- [30] A. Basagni, F. Sedona, C. A. Pignedoli, M. Cattelan, L. Nicolas, M. Casarin, M. Sambri, *J. Am. Chem. Soc.* **2015**, *137*, 1802.
- [31] Q. Sun, L. Cai, Y. Ding, H. Ma, C. Yuan, W. Xu, *Phys. Chem. Chem. Phys.* **2016**, *18*, 2730.
- [32] L. Cai, Q. Sun, C. Zhang, Y. Ding, W. Xu, *Chem. Eur. J.* **2016**, *22*, 1918.
- [33] Q. Sun, L. Cai, Y. Ding, L. Xie, C. Zhang, Q. Tan, W. Xu, *Angew. Chem. Int. Ed.* **2015**, *54*, 4549; *Angew. Chem.* **2015**, *127*, 4632.
- [34] Q. Sun, L. Cai, H. Ma, C. Yuan, W. Xu, *ACS Nano* **2016**, *10*, 7023.
- [35] B. Cirera, Y. Q. Zhang, J. Björk, S. Klyatskaya, Z. Chen, M. Ruben, J. V. Barth, F. Klappenberger, *Nano Lett.* **2014**, *14*, 1891.
- [36] Q. Fan, J. M. Gottfried, J. Zhu, *Acc. Chem. Res.* **2015**, *48*, 2484.
- [37] N. Pavliček, B. Schuler, S. Collazos, N. Moll, D. Pérez, E. Guitián, G. Meyer, D. Peña, L. Gross, *Nat. Chem.* **2015**, *7*, 623.
- [38] B. Schuler, S. Fatayer, F. Mohn, N. Moll, N. Pavliček, G. Meyer, D. Peña, L. Gross, *Nat. Chem.* **2016**, *8*, 220.
- [39] Q. Sun, L. Cai, H. Ma, C. Yuan, W. Xu, *Chem. Commun.* **2016**, *52*, 6009.
- [40] J. van der Lit, F. Di Cicco, P. Hapala, P. Jelinek, I. Swart, *Phys. Rev. Lett.* **2016**, *116*, 096102.
- [41] L. Gross, F. Mohn, N. Moll, P. Liljeroth, G. Meyer, *Science* **2009**, *325*, 1110.
- [42] K. Iwata, S. Yamazaki, P. Mutombo, P. Hapala, M. Ondracek, P. Jelínek, Y. Sugimoto, *Nat. Commun.* **2015**, *6*, 7766.

- [43] Y. He, M. Garnica, F. Bischoff, J. Ducke, M. L. Bocquet, M. Batzill, W. Auwärter, J. V. Barth, *Nat. Chem.* **2017**, *9*, 33.
- [44] K. F. Braun, S. W. Hla, *Nano Lett.* **2005**, *5*, 73.
- [45] F. Klappenberger, D. Kühne, M. Marschall, S. Nepl, W. Krenner, A. Nefedov, T. Strunskus, K. Fink, C. Wöll, S. Klyatskaya, O. Fuhr, M. Ruben, J. V. Barth, *Adv. Funct. Mater.* **2011**, *21*, 1631.
- [46] S. K. Hämmäläinen, N. van der Heijden, J. van der Lit, S. den Hartog, P. Liljeroth, I. Swart, *Phys. Rev. Lett.* **2014**, *113*, 186102.
- [47] N. Moll, L. Gross, F. Mohn, A. Curioni, G. Meyer, *New J. Phys.* **2010**, *12*, 125020.
- [48] A. Riss, A. P. Paz, S. Wickenburg, H. Z. Tsai, D. G. De Oteyza, A. J. Bradley, M. M. Ugeda, P. Gorman, H. S. Jung, M. F. Crommie, A. Rubio, F. R. Fischer, *Nat. Chem.* **2016**, *8*, 678.

Manuscript received: June 15, 2017

Accepted manuscript online: August 3, 2017

Version of record online: August 28, 2017